สถาบันวิจัยแสงซินโครตรอน (องค์การมหาชน)
Synchrotron Light Research Institute (Public Organization)
เอกสารความรู้ (knowledge documents)

ประเภทเอกสาร

- ☑ TR: รายงานเชิงเทคนิค (TECHNICAL REPORT)
- ☐ TN: รายงานเชิงเทคนิค (ฉบับย่อ) (TECHNICAL NOTE)
- ☐ MN: คู่มือการดำเนินงาน (Operation Manual) / คู่มือการใช้งาน (Instruction Manual) / แผนปฏิบัติการ (Operation Plan)

หมายเลขเอกสาร(For QDS) KM Document No.	SLRI-TR-2026-108
ชื่อเรื่อง Title	Proposed Conceptual Design of a 7 MeV Compact Proton Linac at SLRI
ชื่อฝ่าย Department	ฝ่ายวิจัยและพัฒนาเครื่องเร่งอนุภาค
วันที่เผยแพร่ Release date	13 สิงหาคม 2569
ระดับการเปิดเผยข้อมูล Level of Disclosure	☐ ข้อมูลในรายงานเป็นความลับ (Undisclosed)
	☐ เปิดเผยข้อมูลเฉพาะภายในฝ่ายหรือส่วนงาน (Information can be disclosed within department/section)
	☐ เปิดเผยข้อมูลได้สำหรับพนักงานของสถาบันฯ และอนุญาตให้บันทึกข้อมูลเข้าเป็นส่วนหนึ่งของระบบ Knowledge Management ภายในสถาบันฯ (Information can be disclosed for SLRI staffs and can be part of SLRI's Knowledge Management System)
	☑ เปิดเผยข้อมูลได้เพื่อเป็นองค์ความรู้สาธารณะ เช่นเว็บไซต์ของสถาบันฯ (Information is available for public)
คำสำคัญ Keyword	Compact Proton Linac, Fluorine-18, PET Radiotracers, Conceptual Design Report, SLRI, ECRIS, RFQ, IH-DTL

รายชื่อผู้จัดทำรายงานหรือผู้ดำเนินโครงการ **(Name)**	**ส่วนร่วมในการปฏิบัติงานในโครงการ** **Responsible tasks in the project**
ดร.ปรัชญ์ บุญพรประเสริฐ	ดำเนินการศึกษา และจัดทำรายงาน
ดร.ฐกลวรรธน์ จันทร์วัฒนะ	ดำเนินการศึกษา
ดร.สมใจ ชื่นเจริญ	ดำเนินการศึกษา

Proposed Conceptual Design of a 7 MeV Compact Proton Linac at SLRI

Prach Boonpornprasert, Thakonwat Chanwattana, and Somjai Chunjarean
Accelerator Research and Development Division,
Synchrotron Light Research Institute (SLRI), Nakhon Ratchasima, Thailand

13th August 2026

Abstract

This technical report proposes a 7 MeV compact proton linear accelerator for localized Fluorine-18 production at the Synchrotron Light Research Institute (SLRI). To support the conceptual design, the report first reviews the clinical need for PET imaging, the nuclear properties of Fluorine-18, and the architecture of existing compact linac facilities. This local facility is designed to eliminate transit-decay losses when supplying short-lived radiotracers to northeastern Thailand. The proposed 5.5 m beamline layout consists of a permanent-magnet Electron Cyclotron Resonance Ion Source (ECRIS), a Low Energy Beam Transport (LEBT) section, a 325 MHz Radio Frequency Quadrupole (RFQ), an external matching section, and a 325 MHz Interdigital H-mode Drift Tube Linac (IH-DTL). The system delivers a proton beam with a peak current of 18 mA in pulsed mode to meet the current required for isotope production.

Keywords: Compact Proton Linac, Fluorine-18, PET Radiotracers, Conceptual Design Report, SLRI, ECRIS, RFQ, IH-DTL

Declaration: An AI assistant, Gemini, was used for proofreading and language refinement of this report. The authors reviewed and verified all AI-assisted revisions and take full responsibility for the content, analyses, interpretations, and results presented in the report.

Contents

1 Introduction **3**
1.1 Clinical Significance of PET Imaging and Fluorine-18 . . . 3
1.2 Regional Demand and the Strategic Role of SLRI . . . 5
1.3 Objectives . . . 6

2 Concepts, Theories, and Principles **7**
2.1 Nuclear Physics of Fluorine-18 Generation . . . 7
2.2 Transition from Cyclotrons to Linear Accelerators . . . 9
2.3 Fundamental Subsystems of Compact Proton Linacs . . . 10
2.3.1 Electron Cyclotron Resonance Ion Source (ECRIS) . . . 10
2.3.2 Radiofrequency Quadrupole (RFQ) . . . 11
2.3.3 Alvarez Drift-Tube Linac (DTL) . . . 13
2.4 Defining the Extraction Energy . . . 13

3 Methodology **14**

4 Results and Discussion **15**
4.1 Global Benchmarks in Compact Proton Linacs . . . 15
4.1.1 The APTF Injector . . . 15
4.1.2 AccSys PULSAR System . . . 16
4.1.3 The LINAC 7 Project . . . 17
4.1.4 The iBNCT Facility . . . 18
4.1.5 The D-BNCT Facility . . . 18
4.1.6 Comparison of Compact Proton Linac Facilities . . . 19
4.2 Proposed SLRI Linac Facility Architecture . . . 19
4.2.1 Proposed Conceptual Layout of the 7 MeV Baseline . . . 19
4.2.2 Proton Generation: The ECR Ion Source (ECRIS) . . . 20
4.2.3 Low Energy Beam Transport (LEBT) and Injection . . . 21
4.2.4 Radio Frequency Quadrupole (RFQ) . . . 22
4.2.5 External Matching Section . . . 22
4.2.6 Interdigital H-mode Drift Tube Linac (IH-DTL) . . . 22
4.2.7 Linac Baseline Specifications . . . 23
4.2.8 Beam Diagnostics and Instrumentation . . . 25
4.2.9 Upgrade Path for High-Yield Isotope Production . . . 25

5 Conclusion **26**

6 Target Users of the Report **26**

1 Introduction

1.1 Clinical Significance of PET Imaging and Fluorine-18

Positron Emission Tomography (PET) is a highly sensitive medical imaging technique that lets doctors see the actual biological and metabolic functions happening inside the body. While traditional scans like X-rays or CT scans primarily take pictures of physical structures (like bones or the shape of an organ), PET scans are unique because they show how cells are actively behaving, such as how fast they are consuming energy.

To make this happen, a patient is given a safe, tiny amount of a radioactive substance known as a ”radiotracer”. The radioactive atoms in this tracer decay by releasing a positively charged particle called a positron (an antimatter electron). Once released into the tissue, the positron travels a tiny distance before colliding with a standard negative electron. When these two opposites collide, they destroy each other in a process called ”annihilation”. This event converts their mass into pure energy, creating two identical gamma-ray photons that shoot out of the body in exactly opposite directions [1], as illustrated in Figure 1.

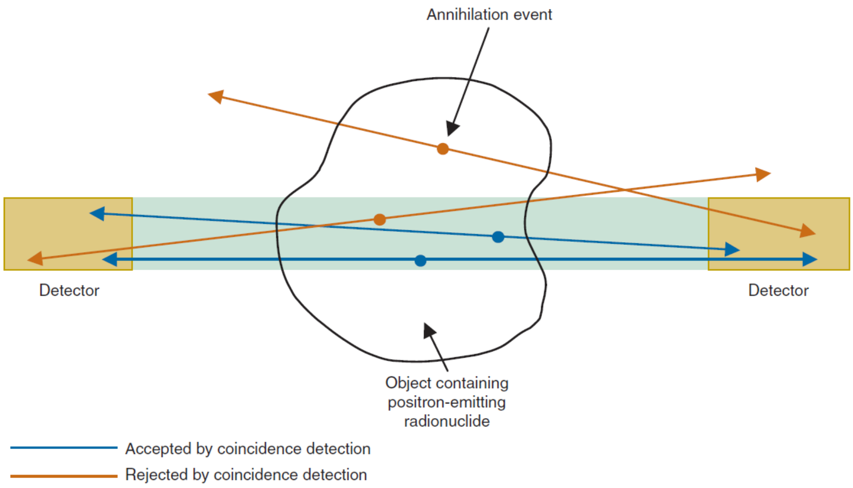

Figure 1: Schematic of Annihilation Coincidence Detection in a PET scanner. The highlighted volume (green area) indicates the region where a pair of simultaneously emitted annihilation photons can be detected in coincidence by opposing detectors. Particles that undergo Compton scattering outside this volume or change direction are rejected [1].

The PET scanner consists of a large ring of radiation detectors surrounding the patient (see Figure 2). The machine is designed to look for these paired photons hitting opposite sides of the detector ring at the exact same moment (a concept called Annihilation Coincidence Detection). By drawing a straight line between the two activated detectors, the computer knows exactly where the original decay happened. By recording millions of these events, the system builds a highly detailed 3D picture of where the tracer is accumulating in the body.

In Thailand, an exemplary facility for advanced molecular imaging is the National Cyclotron and PET Centre at Chulabhorn Hospital [2]. This institution operates state-of-the-art diagnostic equipment, including the Digital PET/CT Biograph Vision (as shown in Figure 3) and the PET/MRI Biograph mMR 3 Tesla. Furthermore, the center plays a crucial national role in medical isotope production by operating its own cyclotron. This cyclotron is dedicated to manufacturing various radiopharmaceuticals, which are essential for PET imaging and are

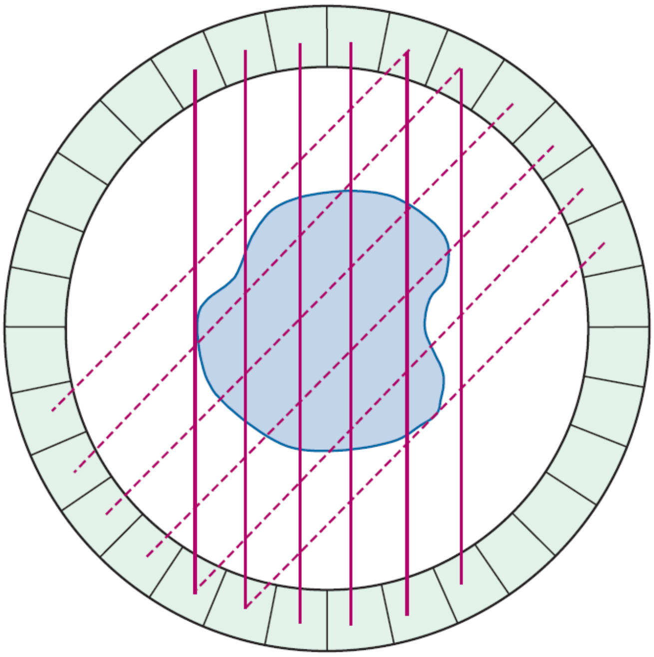

Figure 2: Cross-sectional diagram of a PET detector ring array. The detectors operate in electronic coincidence with those on the opposite side of the ring, a configuration that enables the simultaneous acquisition of projection views from multiple angles [1].

supplied not only for the center's own patients but also distributed to other hospitals across the country.

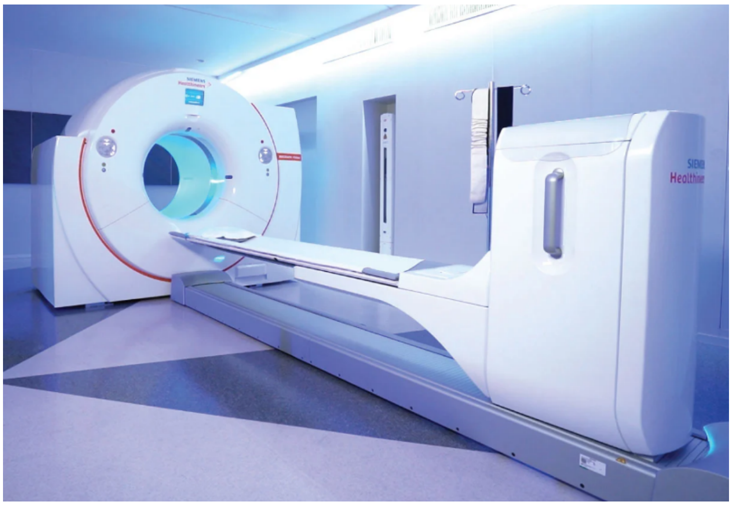

Figure 3: The Siemens Healthineers Digital PET/CT Biograph Vision system utilized for advanced molecular imaging at the National Cyclotron and PET Centre, Chulabhorn Hospital [2].

While several different radioactive isotopes can be used as radiotracers in PET scans, Fluorine-18 (F-18) is the most successful and widely used in clinical settings for three main reasons:

- **Practical half-life:** F-18 has a half-life of 109.8 minutes (the fundamental decay properties of which are detailed further in Section 2.1). This provides enough time to produce the isotope in an accelerator (discussed in Section 2.1), bind it to a biological molecule, transport it to local hospitals, and scan the patient. However, it is also short enough that the radioactivity quickly fades away, keeping the total radiation dose to the patient very low and safe.
- **Short positron range:** When F-18 decays, it releases a low-energy positron, as outlined in Section 2.1. Because of this, the positron travels only about 0.2 mm through tissue before annihilating with an electron. This short range provides sub-millimeter precision, resulting in sharp, high-resolution images with minimal blurring.
- **Chemical substitution:** Fluorine can substitute for specific atoms in biological molecules. It is commonly attached to a sugar molecule to create F-18 FDG, a radioactive form of glucose. Cancer cells, the brain, and the heart naturally consume large amounts of glucose. Because F-18 FDG acts like glucose, it gathers in these areas, allowing doctors to locate tumors and check for brain or heart diseases.

1.2 Regional Demand and the Strategic Role of SLRI

Medical imaging is a critical tool for giving patients the best chance to overcome life-threatening illnesses. In Thailand, functional imaging with PET and Single Photon Emission Computed Tomography (SPECT) plays a vital role in the diagnosis and clinical management of complex conditions, including oncology and chronic neurological syndromes [3].

Despite this clinical importance, advanced PET imaging remains difficult for many patients to access. Currently, there are more than 30 nuclear medicine departments operating across the country [4]. However, a recent 2024 nationwide survey of these facilities showed a stark contrast in equipment usage: hospitals reported 4,641 general SPECT examinations compared to only 409 PET examinations [4]. This bottleneck highlights that while standard nuclear medicine is growing, PET capacity is quite limited.

To expand PET access, hospitals need a steady, daily supply of radioactive tracers. The most common tracer for oncology in Thailand is F-18 FDG (^{18}F-FDG) [4]. While other medical isotopes (such as C-11 or O-15) exist, their extremely short half-lives (under 20 min) make them impossible to transport. This physical limitation leaves F-18 tracers, leveraging the isotope's roughly 110 min half-life, as the primary choice for most hospitals.

While securing this supply is a national challenge, it is especially urgent for regional medical hubs like Nakhon Ratchasima (Korat). As the primary gateway to northeastern Thailand, Korat supports a growing network of wellness centers and hospitals that require advanced PET diagnostics. However, relying on F-18 tracer shipments from distant commercial cyclotrons, such as those in Bangkok, presents a severe logistical problem. Given the 110 min half-life of F-18, a transportation time of several hours results in significant radioactive decay before the isotopes ever reach the patient. This transit loss limits the number of daily PET scans regional hospitals can perform and drastically increases the cost per usable dose.

Developing a localized, linac-based production facility directly in Korat can solve this logistical problem. Furthermore, Korat is uniquely positioned to solve this problem. The province already has a high level of expertise in advanced accelerator physics and beam dynamics at the Synchrotron Light Research Institute (SLRI). This local scientific foundation ensures that a prototype linac facility can be effectively engineered, maintained, and optimized locally, creating a self-sufficient, high-quality medical imaging infrastructure for northeastern Thailand.

1.3 Objectives

The primary goal of this technical report is to establish the baseline layout for a localized medical isotope production facility at SLRI. To achieve this, the report focuses on the following core objectives:

- **Establish the clinical necessity:** Detail the medical demand for Fluorine-18 in northeastern Thailand and explain how local production eliminates radioactive transit losses.
- **Evaluate proven technologies:** Review the operational parameters and physical layouts of existing compact linear accelerators to determine a practical beam energy and facility configuration.
- **Define the baseline layout:** Propose the complete conceptual layout for a 7 MeV compact proton linac, specifying the sequence of core components required for particle generation and acceleration.
- **Ensure future scalability:** Provide a clear, modular upgrade path to increase the final beam energy, allowing the facility to scale up isotope yields as regional medical demand grows.

2 Concepts, Theories, and Principles

2.1 Nuclear Physics of Fluorine-18 Generation

The decay characteristics of Fluorine-18 (F-18) are documented in the dataset provided under the "Nuclear Data" tab of the IAEA Medical Portal [5]. As shown in Figure 4, the downward arrow pointing to the right is a β^+ decay, visually tracking the drop in atomic number from Fluorine ($Z = 9$) to Oxygen ($Z = 8$). This process is the foundation of PET scans used in medical imaging. The key metrics and their physical meanings are described below:

- **Reaction Formula (^{18}O(p, n)^{18}F):** This describes how the isotope is made. A stable Oxygen-18 nucleus is hit with a proton (p), which knocks out a neutron (n) and transforms the atom into Fluorine-18.
- **Half-life (109.77 min):** This is the time it takes for half of the radioactive F-18 atoms in a sample to decay. For medical uses, roughly 110 min is ideal. It is long enough to prepare the dose and scan the patient, but short enough that the radioactivity quickly leaves the body.
- **Decay Mode (β^+ : 100 %):** The isotope decays 100 % of the time via **positron emission** (also known as β^+ decay). The F-18 nucleus releases a positron, turning a proton into a neutron and changing the atom back into stable Oxygen-18 (O-18).
- **Spin and Parity ($1/2^-$):** The $1/2^-$ label next to both F-18 and O-18 represents the quantum state (spin and parity) of the nuclei. Because both the starting and ending nuclei share the exact same quantum state properties, this decay is highly favorable and happens directly without getting stuck in intermediate energy steps.
- **Main Gamma Line (511 keV at 193.8 %):** The intensity exceeds 100 % because each positron annihilation event produces two gamma-ray photons.
  - When the nucleus emits a positron (β^+), that positron almost instantly collides with a nearby electron in the surrounding matter.
  - When matter meets antimatter, they annihilate each other and convert their mass entirely into energy, creating **two** gamma-ray photons traveling in opposite directions.
  - Each photon has exactly 511 keV of energy. Because one single decay event produces a pair of photons, the theoretical yields are doubled ($2 \times 100\,\% = 200\,\%$). The actual measured intensity is 193.8 %, which accounts for a tiny fraction of positrons that escape or undergo alternative interactions.

The efficiency of F-18 production, as illustrated in Figure 5, is presented in the graph available under the "Recommended" tab of the IAEA Medical Portal [5]. It demonstrates the optimal energy required for incoming protons to successfully convert Oxygen-18 into Fluorine-18. The following breakdown explains the key components of the graph:

- **The Axes:** The horizontal x-axis shows the energy (or speed) of the incoming protons, measured in Mega electron-volts (MeV). The primary vertical y-axis on the left shows the "cross section" in millibarns (Note: The millibarn (mb) is a unit of area used in nuclear physics to quantify reaction probabilities, where $1\text{ mb} = 10^{-3}\text{ b} = 10^{-27}\text{ cm}^2$). The cross section represents the probability of the reaction occurring; a higher value indicates a greater chance that a proton will successfully interact with the nucleus to create F-18.

$^{18}O(p,n)^{18}F$

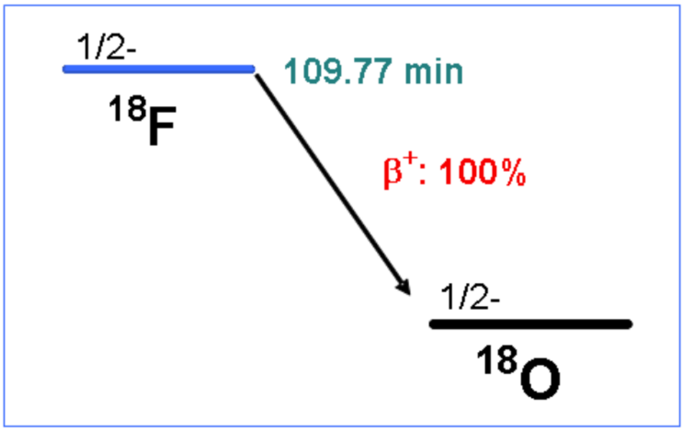

Half-life:	109.77 min
Decay mode:	β^+ 100 %
Main gamma line(s):	511 keV (193.8 %)
More details are at:	http://www.nndc.bnl.gov/nudat2/

Updated: Sep. 2021.

Figure 4: Nuclear decay scheme of F-18 to O-18 via β^+ decay, indicating a half-life of 109.77 min and a primary annihilation radiation line at 511 keV [5].

- **The Data Points and Red Line:** The scattered markers (dots, triangles, and diamonds) represent decades of real-world experimental measurements. To account for the natural scatter in this raw data, a mathematical model is used to draw a “line of best fit” (the solid red line, labeled Padé 98). This curve serves as the official standard that experts rely on for calculations.
- **The Peak:** A prominent spike occurs at approximately 5 MeV. This is the ideal energy level where the O-18 nucleus is perfectly tuned to capture a proton. In practical applications, a medical cyclotron typically fires protons into a water target at a higher starting energy (such as 18 MeV). As the protons travel through the water, they slow down. When their energy drops through the 5 MeV mark, they hit this peak, resulting in maximum F-18 production for PET scans.
- **The Blue Dashed Line (Uncertainty):** This step-like line tracks the statistical confidence in the red standard curve. Its value corresponds to the percentages on the right-side y-axis. Near the highly important 5 MeV peak, the uncertainty is very low (about 5 % to 6 %). At much higher energies (such as 20 MeV), the uncertainty increases to approximately 13 % to 14 %, indicating that the estimates are less reliable in that range.

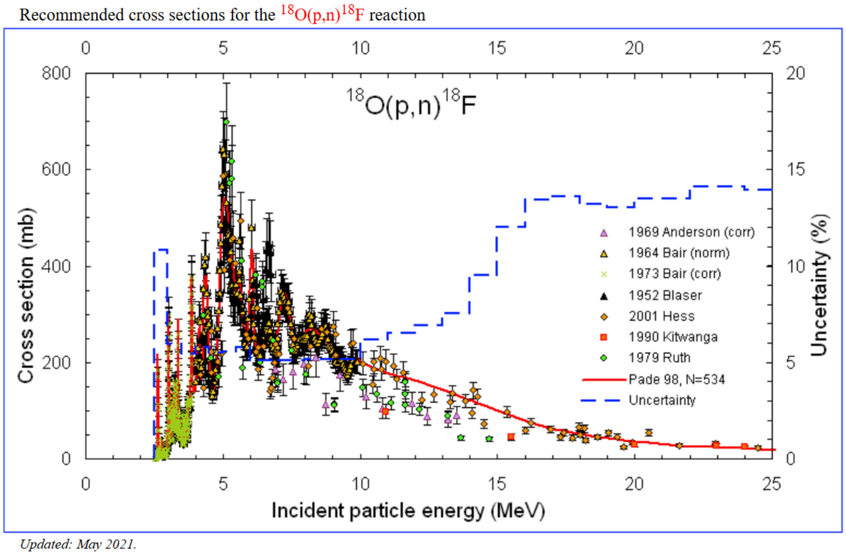

Figure 5: Recommended cross sections and historical experimental data for the $^{18}\mathrm{O(p,n)}^{18}\mathrm{F}$ reaction as a function of incident proton energy [5].

2.2 Transition from Cyclotrons to Linear Accelerators

Designing an accelerator for F-18 production combines machine design with nuclear physics. To ensure a high yield and reliable operation, the design process must select the accelerator type, review the physical limits of the target, and determine the final beam energy.

Cyclotrons are commonly used for medical isotope production because of their compact size [6]. However, they face operational limits when higher yields are required. Major issues include space-charge effects during low-energy injection at the central region and the need for carbon stripping foils for beam extraction. These foils degrade quickly from heat, which requires frequent maintenance and causes radiation buildup inside the machine.

Linear accelerators (linacs) provide a reliable alternative that avoids these issues. A linac separates beam generation, initial capture, and final acceleration, allowing each stage to be optimized. The proposed linac design consists of three main components:

- **Electron Cyclotron Resonance Ion Source (ECRIS):** The ECRIS generates the proton (H^+) beam. It uses microwave heating and magnetic confinement to create a plasma instead of using consumable filaments [7]. This design prevents cathode burnout and allows for stable, high-current operation in continuous or pulsed modes with minimal maintenance.

- **Radio Frequency Quadrupole (RFQ):** The RFQ focuses, bunches, and accelerates the low-velocity beam from the ECRIS [8]. It manages strong space-charge forces at low energies, avoiding the central region limitations found in cyclotrons. The RFQ captures the beam and accelerates it to intermediate energies (typically 3 MeV to 5 MeV) with minimal particle loss [9].

- **Drift Tube Linac (DTL):** The DTL accelerates the bunched protons from the RFQ to the final target energy. Its modular cavities can be tuned to provide specific beam energies for F-18 production. The linear trajectory eliminates the need for stripping foils, allowing for direct beam delivery to the target and reducing residual radiation [10].

Determining the final beam energy for F-18 production depends on the physical limits of the target station. The design must account for production constraints and standard empirical data [6]:

- **Target Chamber Materials:** The target chamber must withstand intense proton bombardment and the highly reactive F-18. Modern, high-yield facilities typically use niobium or tantalum. These materials prevent F-18 from sticking to the walls, ensuring a high recovery rate.
- **Isotopic Contamination Risks:** The target water requires a high O-18 concentration (typically 95 %). If the purity drops, the proton beam interacts with standard O-16. This triggers the $^{16}O(p,\alpha)^{13}N$ reaction and creates Nitrogen-13 contamination. Strict water quality control is necessary to prevent this.
- **Isolation Window Energy Loss:** The beam passes through a thin metal vacuum foil (such as Havar or Niobium) before striking the target. This barrier reduces the beam energy by 1.0 to 2.0 MeV [11]. The linac must provide additional initial energy to compensate for this loss.

2.3 Fundamental Subsystems of Compact Proton Linacs

Compact proton linacs worldwide use a standard architecture to deliver stable, high-current beams within a small footprint, as will be reviewed in Section 4.1. This architecture consists of three main components. The following subsections explain how these machines generate the proton beam and accelerate it to the final extraction energy.

2.3.1 Electron Cyclotron Resonance Ion Source (ECRIS)

The Electron Cyclotron Resonance Ion Source (ECRIS) reliably produces stable, continuous beams of positive ions. The operational sequence in this section follows the framework by Thuillier [12]. Although the internal plasma physics is complex [13, 14], the basic operation consists of three steps: trapping, heating, and extracting particles.

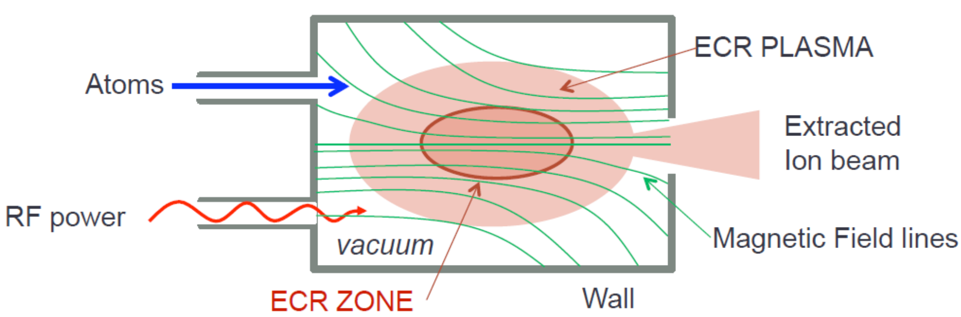

Figure 6: Conceptual schematic of an Electron Cyclotron Resonance Ion Source (ECRIS) [12], illustrating the core components: neutral atom injection, microwave RF heating, magnetic field confinement, the resulting ECR plasma zone, and the extracted ion beam.

As illustrated by the labels in Figure 6, the generation of an ion beam within an ECRIS relies on five fundamental steps:

1. **Creating the Environment (*vacuum*, *Wall*, and *Atoms*):** The process begins inside a metal chamber (the **Wall**) maintained at a very high **vacuum**. A small amount of neutral gas (labeled as **Atoms**, the target material to be ionized) is continuously fed into the chamber. The high vacuum is crucial because it ensures that once atoms become ionized, they do not accidentally collide with stray gas molecules and lose their electrical charge before they can be extracted.

2. **The Magnetic Trap (*Magnetic Field lines*):** To hold the gas in place once it transitions into a plasma, a specialized "magnetic bottle" is created. This invisible trap is formed by a combination of axial and radial magnets. This structure forces charged particles to spiral continuously along the **Magnetic Field lines** rather than hitting the chamber walls.

3. **Microwave Heating (*RF power* and *ECR ZONE*):** Microwave energy (**RF power**) is transported into the chamber. Because of the specific shape of the magnetic bottle, there is a geometric boundary inside the chamber (the **ECR ZONE**) where the frequency of the microwaves perfectly matches the natural spiraling frequency of the electrons. When electrons pass through this exact zone, they absorb energy directly from the microwaves, accelerating to extremely high speeds.

4. **Creating the Plasma (*ECR PLASMA*):** These super-heated, fast-moving electrons bounce back and forth inside the magnetic trap, frequently colliding with the injected neutral gas atoms. When a high-energy electron strikes an atom, it knocks away one of the atom's orbital electrons. This leaves the atom with a net positive charge, turning it into an ion. Because the particles are trapped, this process repeats rapidly, stripping away multiple electrons to create a glowing cloud of highly charged ions (the **ECR PLASMA**).

5. **Extracting the Beam (*Extracted Ion beam*):** While the electrons are incredibly hot and fast, the heavier ions remain relatively slow and "cold". The magnetic trap is deliberately designed to be slightly weaker at one end of the chamber. Ions that randomly drift into this weaker zone escape the magnetic confinement. High-voltage electrodes placed just outside this exit physically pull the positively charged ions out of the plasma, shaping them into a focused, usable **Extracted Ion beam** for the linear accelerator.

2.3.2 Radiofrequency Quadrupole (RFQ)

The Radiofrequency Quadrupole (RFQ) is a specialized linear accelerator structure primarily used to accelerate ion beams at very low velocities, typically between 0.01 and 0.06 times the speed of light [15]. It is exclusively an ion accelerator, as electron sources emit particles at much higher initial velocities.

At these extremely low particle velocities, conventional magnetic lenses are highly inefficient, but electric forces remain strong. The RFQ utilizes velocity-independent electric fields to provide a strong-focusing advantage. As illustrated in Figure 7, the structure relies on four conducting electrodes (referred to as rods or vanes) that are mounted symmetrically around the central beam axis. An alternating current (AC) voltage, described by $\pm V_0 \cos(\omega t)/2$, is applied to the four electrodes in a quadrupole pattern. Here, V_0 represents the peak voltage amplitude, ω is the angular frequency of the radio frequency (RF) wave, and t represents time. This configuration generates a time-varying electric quadrupole field that continuously confines the beam transversely [15].

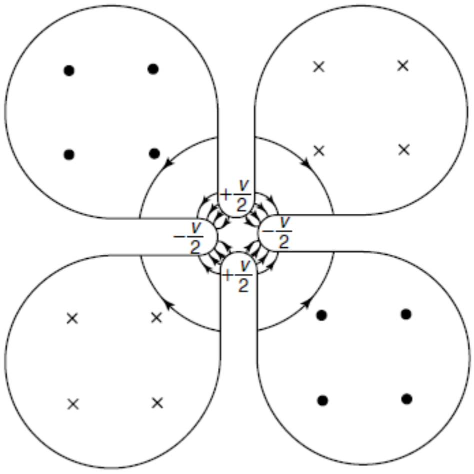

Figure 7: Cross-sectional view of the four-vane RFQ geometry, illustrating the symmetric arrangement of the electrodes that produce the transverse electric quadrupole focusing field [15].

A uniform electrode geometry produces no axial electric field to push the particles forward. To achieve longitudinal acceleration, the transverse distance between the electrode tips and the central axis is modulated along the length of the structure, as depicted in Figure 8. This geometric modulation creates an axial electrical potential, which in turn generates the necessary longitudinal electric field. The spatial period of this modulation is matched exactly to the distance a synchronous particle travels in one RF period [15].

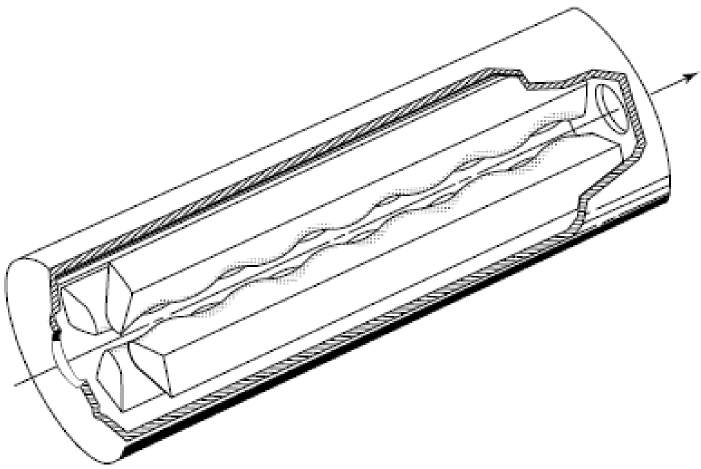

Figure 8: Longitudinal profile of the RFQ vanes. The geometric modulation along the beam axis perturbs the transverse field to create a longitudinal accelerating component [15].

The RFQ eliminates the need for external drift tubes or magnetic quadrupoles by simultaneously focusing, bunching, and accelerating the beam. By slowly varying the structural parameters of the RFQ along its length, the continuous beam from the ion source is adiabatically captured and grouped into stable bunches. This gentle bunching process avoids sudden longitudinal compression, minimizing disruptive space-charge forces and allowing the accelerator to handle much higher beam currents.

2.3.3 Alvarez Drift-Tube Linac (DTL)

The Alvarez Drift-Tube Linac (DTL) accelerates protons and heavier ions from the RFQ through a medium-velocity range, typically 0.04 to 0.4 times the speed of light [15].

To prevent particles from decelerating when the alternating RF electric field reverses, hollow conducting drift tubes are placed along the central axis of the cavity (Figure 9). The electric field decays to zero inside these tubes. Particles are shielded during the decelerating phase of the RF cycle and cross the gaps between tubes during the accelerating phase.

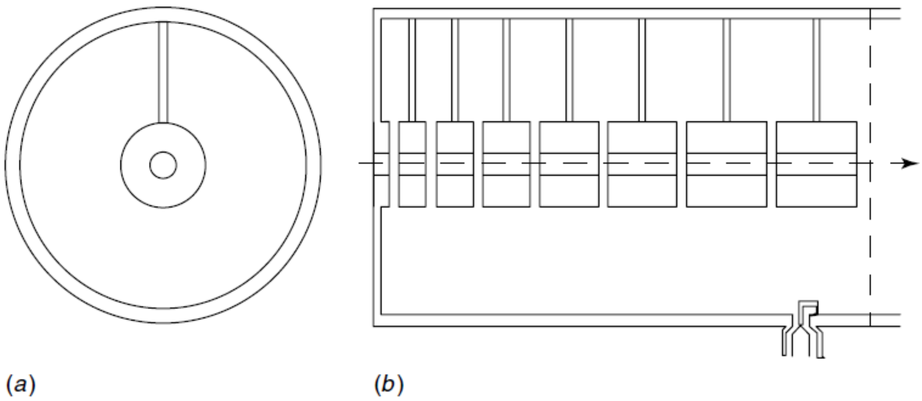

Figure 9: Schematic of the Alvarez Drift-Tube Linac (DTL). (a) Transverse cross-section showing a central drift tube suspended by a support stem within the cylindrical resonant cavity. (b) Longitudinal cross-section illustrating the sequence of drift tubes. Tube lengths increase progressively to accommodate the increasing particle velocity [15].

The DTL cavity is divided into individual accelerating cells, extending from the center of one drift tube to the next. The nominal cell length is $\beta\lambda$, where β is the relative particle velocity and λ is the RF wavelength. The electric fields in all cells oscillate in phase, meaning the multicell structure operates in a "zero mode."

To maintain tight control over the beam profile as it accelerates, magnetic quadrupole lenses are installed directly inside the hollow drift tubes to provide continuous transverse focusing. The open internal structure of the DTL, which lacks separating end-walls between cells, yields a high effective shunt impedance. However, this efficiency drops at higher particle velocities. Because the cell length ($\beta\lambda$) increases as the particles speed up, the gaps between the drift tubes must also become longer. These extended gaps reduce the transit-time factor and ultimately lower the effective shunt impedance of the machine at higher energies.

2.4 Defining the Extraction Energy

The DTL extraction energy is determined by nuclear physics parameters and production yield requirements:

- **Reaction Cross-Section:** The $^{18}O(p,n)^{18}F$ excitation function has a maximum cross-section exceeding 600 mb at approximately 5.1 MeV [5]. The optimal interaction window spans 4 MeV to 7 MeV.

- **Foil Energy Loss:** The beam loses 1.0 to 2.0 MeV when traversing the isolation foil. The DTL must deliver a higher initial energy so the beam enters the target fluid above the

5.1 MeV peak, sustaining isotope production as the beam decelerates through the optimal window.

- **Thick-Target Yield:** Experimental data compiled by the IAEA [6] demonstrates that isotope yield scales significantly with incident beam energy (Table 1). These reference values for $^{18}O(p,n)^{18}F$ assume a target volume—typically enriched water ($H_2^{18}O$) or oxygen gas ($^{18}O_2$) housed within a silver, niobium, or tantalum chamber—that is physically thick enough to degrade the incident proton beam down to 2.5 MeV, near the reaction threshold. At a lower incident energy of 8 MeV, the yield is 132 mCi/µA (4.9 GBq/µA). A beam entering the target at 11 MeV yields approximately 230 mCi/µA (8.5 GBq/µA). Increasing the extraction energy to 18 MeV yields roughly 373 mCi/µA (13.8 GBq/µA), an approximate 60 % increase over the 11 MeV beam and nearly triple the yield of the 8 MeV configuration.

Table 1: Thick target yields of $^{18}O(p,n)^{18}F$ [6].

Energy range (MeV)	F-18 yield at saturation (mCi/µA)	F-18 yield at saturation (GBq/µA)
20–2.5	395	14.6
18–2.5	373	13.8
15–2.5	327	12.1
11–2.5	230	8.5
8–2.5	132	4.9

Selecting the final extraction energy requires balancing absolute isotope yield against physical facility constraints. As demonstrated by the yield data, extraction energies in the 11 MeV to 18 MeV regime are optimal for maximizing absolute isotope production. However, achieving these higher energies necessitates a long DTL structure, greater RF power consumption, and substantially thicker radiation shielding due to increased secondary neutron production.

Conclusion on Energy Selection: While the 11 MeV to 18 MeV range provides the highest production yield, lower extraction energies between 7 MeV to 8 MeV offer significant architectural and operational advantages. Despite a lower total yield, a 7 MeV to 8 MeV linac provides a highly compact footprint that drastically reduces facility shielding requirements and prevents high-energy parasitic reactions. Furthermore, after accounting for the 1.0 to 2.0 MeV energy loss through the isolation window, a 7 MeV to 8 MeV beam still enters the target aligned with the 5.1 MeV resonance peak of the $^{18}O(p,n)^{18}F$ reaction. Therefore, the final design energy must be selected based on the specific footprint constraints and capacity goals of the intended facility.

3 Methodology

Developing the conceptual design for the SLRI proton linac relies on a straightforward, two-step process. First, the report reviews the layouts and operational parameters of several established compact proton linac facilities. Second, the operational data gathered from these benchmark systems is used to design the proposed beamline. This includes determining the specific sequence of core components and setting their baseline physical specifications. The benchmark review and the final proposed layout are discussed in the following section.

4 Results and Discussion

4.1 Global Benchmarks in Compact Proton Linacs

To establish a baseline for the design parameters and operational capabilities of the proposed system, it is essential to evaluate the landscape of modern, low-energy proton linear accelerators. Globally, several facilities have successfully developed and commissioned compact room-temperature linacs for applications ranging from hospital-based isotope production to neutron generation and advanced hadron therapies. This section provides a comparative review of five prominent benchmark configurations.

4.1.1 The APTF Injector

The Advanced Proton Therapy Facility (APTF), developed by the Shanghai Institute of Applied Physics (SINAP), utilizes a compact, room-temperature linear injector designed for synchrotron-based proton therapy [16]. The injector is designed to accelerate an 18.0 mA proton beam to a final energy of 7.0 MeV. As illustrated in Figure 10, the overall beamline layout consists of an electron cyclotron resonance ion source (ECR-IS), a low energy beam transport (LEBT) line, a Radio Frequency Quadrupole (RFQ), an external matching section, and an interdigital H-mode Drift Tube Linac (IH-DTL).

The total footprint of the injector system is approximately 5 m, spanning from the exit of the ECR to the exit of the DTL. This length is predominantly occupied by the 3.01 m RFQ and the 0.82 m IH-DTL, while the remaining space accommodates the LEBT and the external matching section.

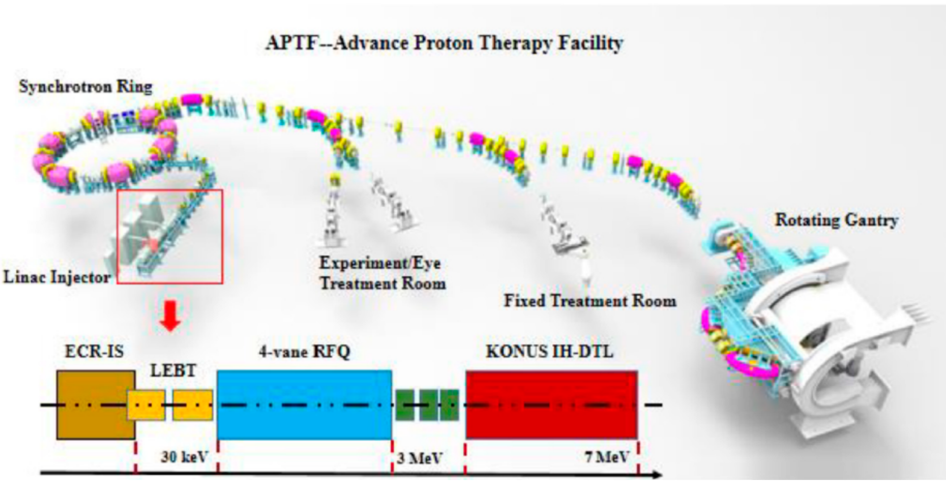

Figure 10: Overall layout of the APTF injector beamline [16].

Following the LEBT, the proton beam is injected into a four-vane RFQ operating at 325 MHz. The RFQ employs a fast-bunching strategy to accelerate the protons to 3.0 MeV. The structure is specifically optimized to prevent parametric resonance (a condition where coupling between the longitudinal and transverse beam oscillations leads to severe emittance growth and beam loss). By continuously profiling the vane modulation and aperture along the length of the RFQ, the design maintains a safe separation between the transverse and longitudinal phase advances. The beam then transitions from the RFQ into the IH-DTL through a compact external quadrupole triplet matching section.

The DTL utilizes modified Kombinierte Null Grad Struktur (KONUS) beam dynamics, which allows for the removal of focusing magnets from inside the cavity to simplify fabrication and maintenance. The structure accelerates the protons up to 7.0 MeV with an accelerating gradient of 4.88 MV/m. Simulation results indicate a transmission efficiency above 95 %, yielding normalized root mean square (RMS) emittances of 0.23π mm-mrad in the transverse plane and 2.216π keV/u-ns longitudinally at the linac exit.

4.1.2 AccSys PULSAR System

An established benchmark for compact proton linear accelerators dedicated to hospital-based positron emission tomography (PET) isotope production is the PULSAR system developed by AccSys Technology [17]. Optimized specifically for F-18 generation, the accelerator layout uses a three-stage design: a 30 keV standard proton ion source, a Radio Frequency Quadrupole (RFQ), and an Alvarez Drift Tube Linac (DTL).

By operating at an RF frequency of 425 MHz, the system maintains a compact accelerating gradient that minimizes the overall cavity dimensions. To align with the $^{18}O(p,n)^{18}F$ reaction cross-section, the machine delivers an output beam energy ranging from 7 MeV to 11 MeV. The system is capable of generating peak currents between 20 mA and 30 mA. By scaling the duty factor during operation, the linac can deliver an average beam current of up to 50 µA to the production target.

The physical layout of the system is constrained to accommodate existing clinical environments. The accelerating structures, which include a 1.59 m RFQ and a 2.81 m DTL, are mounted on a unified alignment box-frame. The total beamline length is approximately 4.5 m, enabling the entire assembly to be housed within a standard 5 m shielded bunker. As depicted in Figure 11, the target station incorporates localized shielding, which serves to reduce the broader radiation containment requirements of the host facility.

Figure 11: The AccSys PULSAR compact proton linac system [17]. The modular assembly shows the ion source and RFQ on the left, followed by the Alvarez DTL, and culminating in the locally shielded target station on the right.

4.1.3 The LINAC 7 Project

The LINAC 7 project is a compact proton accelerator currently under development by the IZPILab-Beam Laboratory at the University of the Basque Country [18]. The system is designed for low-current, low-energy applications, including the potential production of short-lived medical radioisotopes. It is configured to deliver a final proton beam energy of 7 MeV.

The accelerator layout uses a series of radio-frequency structures to capture, focus, and accelerate the proton beam. As shown in Figure 12, the beamline consists of an ion source, a Low Energy Beam Transport (LEBT) section, a Radio Frequency Quadrupole (RFQ), a Medium Energy Beam Transport (MEBT) section, a Drift Tube Linac (DTL), and a beam stop.

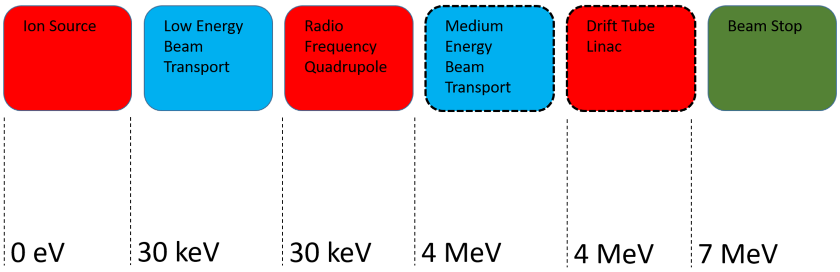

Figure 12: Block diagram of the LINAC 7 accelerator architecture, showing the beam energy progression from 0 eV to 7 MeV [18].

An Electron Cyclotron Resonance Ion Source (ECRIS), shown in Figure 13 (left), generates the particles for the system. The ECRIS produces a proton plasma and extracts the initial beam at 30 keV. Following the LEBT, the RFQ (Figure 13 (right)) captures the 30 keV continuous beam. This structure focuses and accelerates the proton bunches to an intermediate energy of 4 MeV while managing space-charge forces.

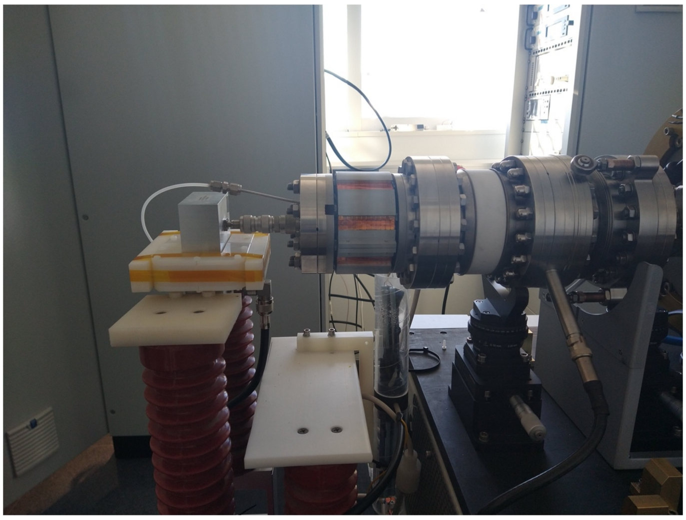

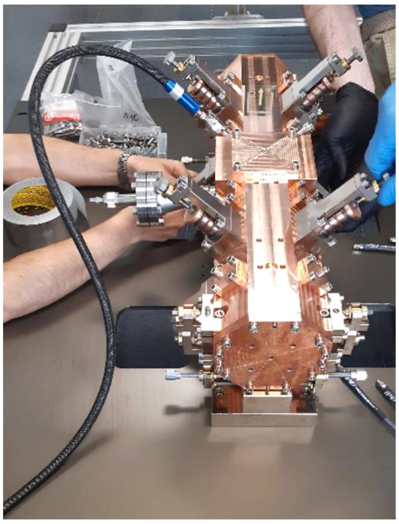

Figure 13: The Electron Cyclotron Resonance Ion Source (ECRIS) used in the LINAC 7 project for proton beam generation (left) and Assembly of the Radio Frequency Quadrupole (RFQ) used to accelerate the proton beam from 30 keV to 4 MeV (right) [18].

4.1.4 The iBNCT Facility

The iBNCT project, led by the University of Tsukuba in collaboration with the High Energy Accelerator Research Organization (KEK) and the Japan Atomic Energy Agency (JAEA), provides a highly relevant architectural reference for compact medical linacs [19]. Although engineered specifically for Boron Neutron Capture Therapy (BNCT), its reliance on a low-energy, high-current proton beam to generate secondary particles closely parallels the physical and operational requirements of linear accelerator-based isotope production.

The accelerator utilizes a Radio Frequency Quadrupole (RFQ) and a Drift Tube Linac (DTL) configuration, as illustrated in Figure 14. A multicusp ion source generates the initial proton beam, which is injected into the RFQ at 50 keV and accelerated to 3 MeV. The beam is subsequently accelerated by the DTL to a final extraction energy of 8 MeV. Both accelerating structures operate at an RF frequency of 324 MHz and are driven by a single klystron. The total footprint of the linac is compact, measuring approximately 8 m in length. While the system was originally designed to support an average proton current of 5 mA, recent operational updates indicate that the facility has achieved stable operation at an average current of 2.1 mA [20].

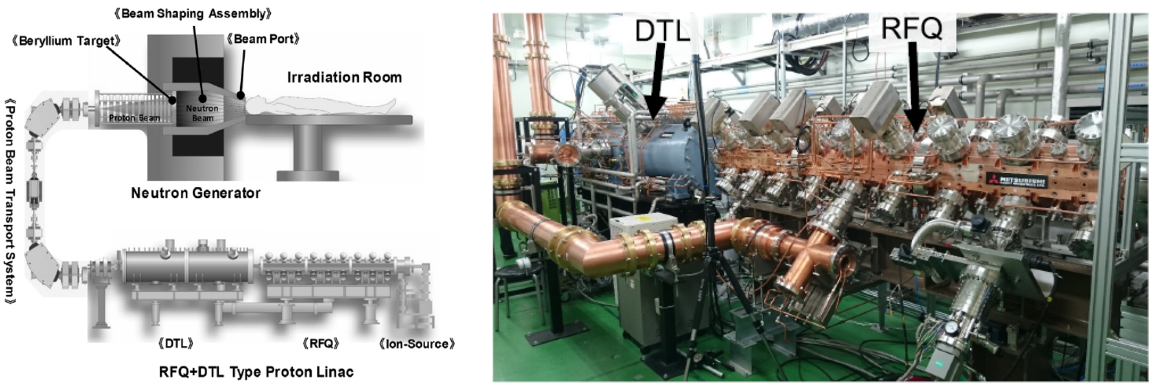

Figure 14: Overview of the iBNCT accelerator. Schematic of the complete linac-based neutron source, including the beam shaping assembly (left) and the actual RFQ and DTL tubes installed in the facility (right) [19].

4.1.5 The D-BNCT Facility

Another example of a compact proton linear accelerator facility in China is the D-BNCT (Dongguan Boron Neutron Capture Therapy) project, developed by the Institute of High Energy Physics (IHEP) of the Chinese Academy of Sciences. Located at the Dongguan campus, the facility is designed as a compact, accelerator-based neutron source specifically for clinical BNCT applications and related experimental research [21].

The accelerator layout of the initial experimental device, D-BNCT01, relies primarily on a Radio Frequency Quadrupole (RFQ) linac. The system accelerates a proton beam to a final extraction energy of 3.5 MeV. The RFQ is optimized to deliver an average proton beam current of 4.5 mA. To generate the required epithermal neutron flux, the 3.5 MeV proton beam is directed onto a fixed lithium target, utilizing the $^{7}\mathrm{Li(p,n)}^{7}\mathrm{Be}$ nuclear reaction. The compact nature of the RFQ and the selected beam parameters are designed to provide sufficient neutron intensity while maintaining a physical footprint suitable for integration into hospital environments.

4.1.6 Comparison of Compact Proton Linac Facilities

To synthesize the parameters discussed in the preceding subsections, Table 2 provides a direct comparison of the architectural and operational characteristics of the reviewed facilities. This summary highlights the diverse approaches taken to achieve stable proton beam delivery within a restricted footprint, validating the design parameters and scale for the proposed linac prototype.

Table 2: Summary of operational parameters and physical footprints of benchmark compact proton linear accelerators.

Facility / System	Beam Energy	Beam Current	Footprint	Primary Purpose
APTF Injector (China)	7.0 MeV	18.0 mA (Peak)	~5 m	Therapy Injector
AccSys PULSAR (USA)	7 MeV to 11 MeV	20 mA to 30 mA (Peak) 50 µA (Avg)	~4.5 m	PET Isotopes
LINAC 7 (Spain)	7 MeV	Low-current	Compact	Radioisotopes
iBNCT Facility (Japan)	8 MeV	2.1 mA (Avg)	~8 m	BNCT
D-BNCT (China)	3.5 MeV	4.5 mA (Avg)	Compact	BNCT

4.2 Proposed SLRI Linac Facility Architecture

4.2.1 Proposed Conceptual Layout of the 7 MeV Baseline

Following the institutional decision to develop a compact proton linac for localized isotope production, SLRI sought a proven architectural baseline to minimize technical risk and optimize initial capital investment. The injector of the Advanced Proton Therapy Facility (APTF) was selected as the primary reference design [16]. By adapting this established framework, the SLRI system is engineered to deliver an 18.0 mA peak proton beam at a final extraction energy of 7.0 MeV.

While previous analyses identified an optimal extraction energy between 11 MeV and 18 MeV to maximize thick-target yields for regional distribution, an initial 7.0 MeV baseline—validated by the APTF's operational parameters—is highly pragmatic for establishing proof-of-concept operations. Furthermore, the modularity of the linear accelerator architecture guarantees a clear upgrade path; the final extraction energy can be increased in future phases by appending additional accelerating tanks in series.

As illustrated in the block diagram in Figure 15, the complete beamline is constrained to a compact footprint of approximately 5.5 m, spanning from the rear of the ion source to the exit of the primary accelerator structure. This spatial efficiency closely mirrors the compact nature of the APTF reference design, making it highly suitable for localized medical integration.

The progression of the proton beam is managed through a sequence of five specialized subsystems, which are detailed in the subsequent sections:

- **Proton Generation (ECRIS):** The beam is generated and extracted at an initial energy of 60 keV.
- **Low Energy Beam Transport (LEBT):** A dual-quadrupole focusing section matches the divergent ECRIS beam into the RFQ acceptance bucket.

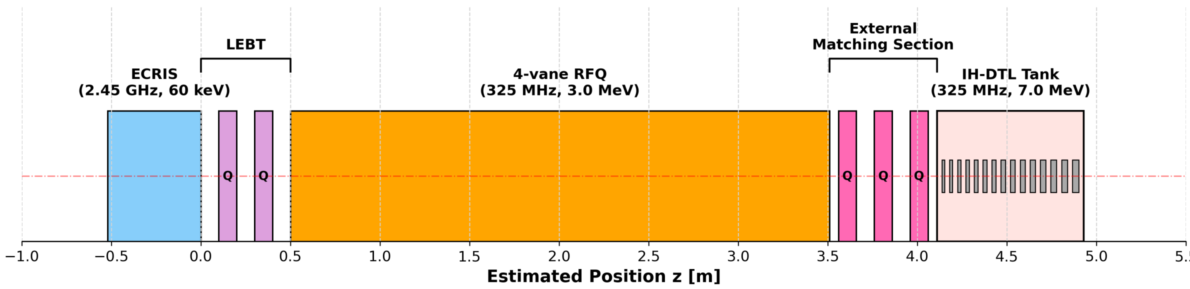

Figure 15: Conceptual block layout of the proposed 7.0 MeV compact proton linac baseline for SLRI. The beamline progresses from the ECRIS on the left, through the LEBT and RFQ, and into the final IH-DTL tank via a compact external matching section.

- **Radio Frequency Quadrupole (RFQ):** The primary 325 MHz bunching and accelerating structure elevates the beam energy to 3.0 MeV.
- **External Matching Section:** A compact external quadrupole triplet provides strict transverse phase-space matching between the RFQ and the DTL.
- **Interdigital H-mode Drift Tube Linac (IH-DTL):** The final accelerating tank brings the matched proton bunches to the 7.0 MeV extraction energy required for the isotope production target.

4.2.2 Proton Generation: The ECR Ion Source (ECRIS)

The foundation of the proposed localized isotope production linac is the initial particle generation system, which utilizes a compact Electron Cyclotron Resonance Ion Source (ECRIS). Specifically, the facility design evaluates the dynamic parameters of the HiQ 60 source-extraction architecture developed by Pantechnik [22]. This selection prioritizes high operational reliability, plasma stability, and minimal maintenance downtime, which are critical for sustaining a continuous medical isotope supply chain.

A simplified layout of the ECRIS configuration is illustrated in Figure 16, highlighting the primary functional zones of the machine adapted from the HiQ 60 design [22].

The assembly comprises three main integration stages:

- **RF Port (Injection):** Located at the rear injection flange, a standard WR340 rectangular waveguide interface connects the source to the microwave power network [22]. This waveguide delivers 2.45 GHz microwave power directly into the internal cavity. The neutral gas input line is integrated alongside this port to feed target atoms directly into the active ionization zone.
- **Gas/Plasma Chamber and Magnetic Confinement System:** The central cylindrical volume contains the vacuum plasma chamber where high-density ionization occurs. To establish the required magnetic gradient for electron cyclotron resonance and plasma stability, the chamber is surrounded by a passive, purely permanent-magnet confinement system. This eliminates the need for active electromagnet coils, significantly reducing the facility's front-end electrical power load and removing complex auxiliary cooling infrastructure.

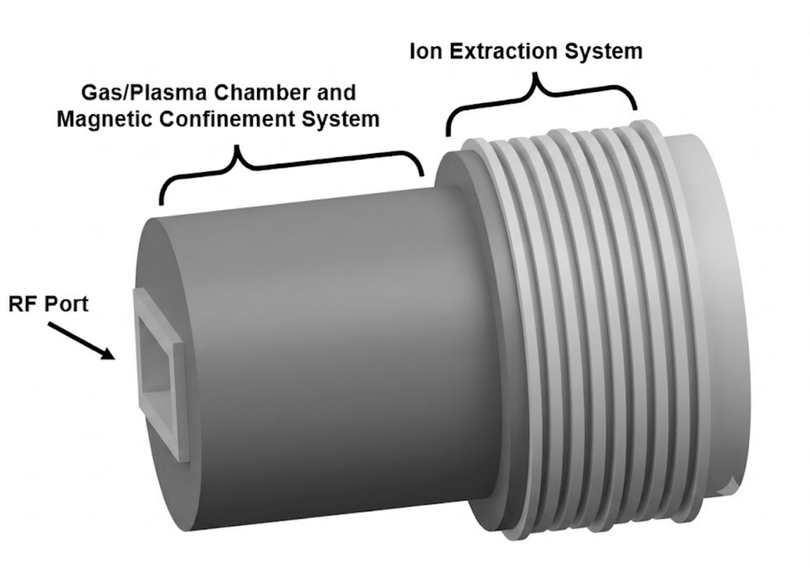

Figure 16: Conceptual schematic of an ECR source and extraction system, based on the architecture of the Pantechnik HiQ 60 [22]. The labeled components illustrate the rectangular RF injection port, the central cylindrical volume housing the plasma chamber and permanent magnetic confinement system, and the multi-electrode high-voltage ion extraction array.

- **Ion Extraction System:** The multi-ring assembly at the forward end houses a specialized high-voltage extraction geometry, incorporating dedicated connections for a repeller and an electrostatic puller electrode [22]. This configuration handles an extraction potential of up to 60 kV, providing strict control over the initial beam optics and effectively managing the space-charge forces inherent to a low-velocity, high-current extraction profile.

The source is engineered to deliver a peak proton (H^+) beam current of up to 50 mA with a normalized root-mean-square (RMS) emittance of $\leq 0.2\,\pi \cdot \text{mm} \cdot \text{mrad}$. To align with the overall thermal management strategy of the compact linac, the system supports low duty-cycle pulsed-mode operation, which drastically mitigates the continuous thermal dissipation burden on the downstream accelerating structures while successfully meeting the average current benchmarks required for clinical radiotracer production.

4.2.3 Low Energy Beam Transport (LEBT) and Injection

The proton beam generated by the HiQ 60 ECRIS is extracted at an initial energy of 30 keV to perfectly align with the injection parameters established by the APTF RFQ baseline [16]. While the ion source is capable of delivering peak currents up to 50 mA, the Low Energy Beam Transport (LEBT) section is optimized to transport and collimate the nominal 18.0 mA beam required for downstream acceleration.

Managing the strong space-charge forces inherent to this high-current, low-velocity regime requires aggressive transverse focusing. The LEBT utilizes a compact double electrostatic quadrupole lens configuration to shape the diverging beam and precisely match the Twiss parameters to the acceptance bucket of the RFQ.

4.2.4 Radio Frequency Quadrupole (RFQ)

The primary accelerating and bunching structure is a four-vane Radio Frequency Quadrupole (RFQ) operating at a frequency of 325 MHz. The RFQ is designed to capture the 30 keV continuous proton beam injected from the LEBT and efficiently accelerate it to an intermediate energy of 3.0 MeV.

To minimize the physical footprint without embarking on a custom, resource-intensive cavity optimization process for this conceptual phase, the design directly adopts the established beam dynamics and fast-bunching strategy of the APTF baseline [16]. By relying on this proven rapid ramping of the modulation factor in the gentle bunching section rather than a traditional adiabatic approach, the total cavity length remains highly compact at just 3.01 m.

The structure is driven by a constant inter-vane voltage of 74.58 kV across its entire length. This voltage profile corresponds to a safe maximum surface electric field, maintaining a Kilpatrick factor of 1.7 to strictly prevent vacuum sparking and ensure reliable operation. Reference beam dynamics simulations for this specific structural configuration demonstrate an excellent transmission efficiency of 98.0 %, successfully delivering the bunched protons to the downstream matching section.

4.2.5 External Matching Section

The external matching section transitions the 3.0 MeV proton beam from the RFQ into the interdigital H-mode Drift Tube Linac (IH-DTL). Its primary purpose is to provide the necessary transverse and longitudinal phase-space matching between these two accelerating structures.

Following the APTF reference design, this matching layout utilizes an external quadrupole triplet to manage transverse focusing. Longitudinally, the system relies on the exit phase shift and energy spread parameters inherent to the RFQ to meet the acceptance requirements of the subsequent DTL. This configuration intentionally omits an independent RF bunching cavity within the matching section.

The specific lattice arrangement, drift lengths, and quadrupole gradients will be defined after dedicated beam dynamics simulations are performed in the subsequent design phase.

4.2.6 Interdigital H-mode Drift Tube Linac (IH-DTL)

The final stage of acceleration is driven by an Interdigital H-mode Drift Tube Linac (IH-DTL) operating at 325 MHz. Unlike the Alvarez DTL described in Section 2.3.3, the IH-DTL uses alternating stems to support the drift tubes. This design makes the cavity smaller and more efficient at low beam energies. Receiving the 3.0 MeV phase-matched proton bunches from the external matching section, the IH-DTL accelerates the beam to the final 7.0 MeV extraction energy required for isotope production.

Following the APTF architectural baseline [16], the design utilizes modified Kombinierte Null Grad Struktur (KONUS) beam dynamics [23]. In this configuration, transverse magnetic focusing lenses are removed from the interior drift tubes and handled entirely by the upstream external quadrupole triplet. This allows the compact 0.82 m cavity to be dedicated strictly to longitudinal beam manipulation.

As illustrated in Figure 17, the internal electromagnetic structure consists of alternating drift tubes (supported by stems on opposite sides of the cavity) that form 15 distinct accelerating gaps. To optimize beam dynamics without internal lenses, the cavity is divided into two operational regimes:

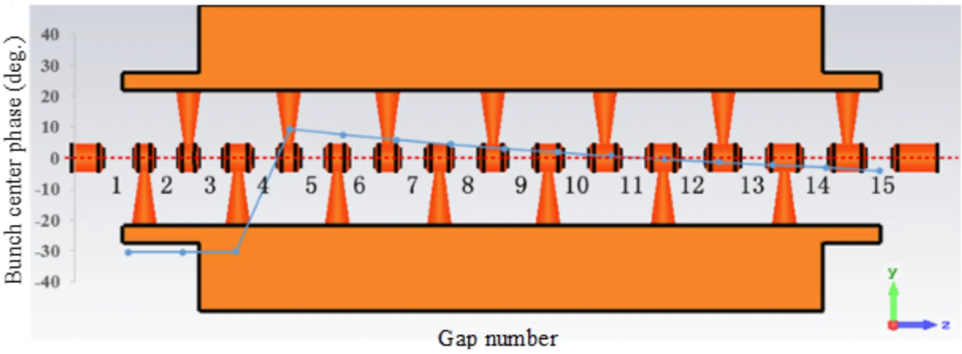

Figure 17: Cross-sectional layout of the IH-DTL cavity, illustrating the alternating drift tube geometry and the synchronous phase at each gap center (adapted from the APTF reference design) [16].

- **Re-bunching Section (Gaps 1–3):** The initial gaps operate at a −30° synchronous phase. This off-crest phase provides longitudinal focusing to tightly bunch the beam as it enters the structure.
- **Accelerating Section (Gaps 4–15):** The remaining gaps transition to operate near a 0° synchronous phase. This on-crest configuration provides the highest accelerating field to efficiently increase the beam energy.

By separating these longitudinal functions, the structure sustains a high average accelerating gradient of 4.88 MV/m. This allows the IH-DTL to successfully deliver the 18.0 mA peak current beam to 7.0 MeV within a minimal physical footprint.

4.2.7 Linac Baseline Specifications

The complete beamline, consisting of the ECR ion source, RFQ, and IH-DTL, is designed to support localized medical isotope production. Based on the APTF reference design, the facility is configured to deliver a 18.0 mA proton beam at 7.0 MeV within a 5.5 m footprint.

The physical and operational parameters for this conceptual design are summarized in Table 3. These values will serve as the baseline for subsequent beam dynamics simulations and mechanical engineering stages.

Table 3: Physical and operational specifications for the proposed SLRI compact proton linac baseline.

Subsystem	Parameter	Design Value
System Overview	Particle Type	H^+
	Final Beam Energy	7.0 MeV
	Nominal Peak Current	18.0 mA
	Total Estimated Length	~5.5 m
Ion Source (ECRIS)	Source Architecture	Permanent Magnet (HiQ 60 type)
	Microwave Driving Frequency	2.45 GHz
	Maximum Extraction Voltage	60 kV
	Output Injection Energy	30 keV
	Maximum Peak Beam Current	50 mA
RFQ	Structure Type	4-vane
	Operating Frequency	325 MHz
	Input Energy	30 keV
	Output Energy	3.0 MeV
	Cavity Length	3.01 m
	Inter-vane Voltage	74.58 kV
	Kilpatrick Factor	1.7
	Reference Transmission Efficiency	98.0 %
IH-DTL	Structure Type	IH-mode (Modified KONUS)
	Operating Frequency	325 MHz
	Input Energy	3.0 MeV
	Output Energy	7.0 MeV
	Cavity Length	0.82 m
	Number of Gaps	15 (3 Bunching, 12 Accelerating)
	Average Accelerating Gradient	4.88 MV/m

4.2.8 Beam Diagnostics and Instrumentation

To ensure stable beam delivery and validate the phase-space matching between the accelerating structures, a comprehensive suite of beam diagnostics is required. Drawing from the diagnostic layouts of benchmark facilities such as the LINAC 7 project [18], the instrumentation is concentrated primarily within the low-energy transport line and the external matching section to preserve the overall compact footprint of the facility. The baseline diagnostic configuration proposes the following options [24]:

- **AC Current Transformers (CT):** Non-destructive toroidal monitors used to continuously measure the macroscopic pulsed beam current and monitor transmission efficiency. *Installation:* Positioned at the LEBT exit, the external matching section, and immediately following the DTL extraction window.
- **Faraday Cups (FC):** Destructive, water-cooled interceptive blocks used for absolute beam current calibration and as temporary beam stops during initial source tuning. *Installation:* Housed within a localized diagnostic box in the LEBT and at the final extraction point prior to the target.
- **Scintillating Screen Stations:** Insertable, destructive monitors used to measure the transverse beam profile and spatial alignment. *Installation:* Integrated into the LEBT and external matching section to verify the Twiss parameters entering the RFQ and DTL, respectively.
- **Pepper-Pot Emittance Scanner:** A specialized mechanical mask and screen assembly used to directly measure the 4D transverse phase space of the low-energy, space-charge-dominated beam. *Installation:* Temporarily installed in the LEBT diagnostic box during the commissioning phase to optimize the ECRIS extraction optics.
- **Dipole Spectrometer:** A magnetic analysis bending magnet used to measure the initial beam momentum spread and verify the proton fraction against unwanted ion species. *Installation:* Temporarily installed directly after the ECRIS strictly for the initial source commissioning phase.
- **Time-of-Flight (ToF) Monitors:** Non-destructive capacitive phase probes used to accurately measure the beam velocity and absolute longitudinal energy spread. *Installation:* Configured as a pair within the external matching section drift space and at the exit of the DTL.

It should be noted that the devices listed above represent a preliminary suite of diagnostic options. The final selection, physical integration, and specific spatial layout of these instruments will be determined following dedicated beam dynamics simulations and engineering studies in the subsequent design phase.

4.2.9 Upgrade Path for High-Yield Isotope Production

The initial 7.0 MeV baseline validates the core architecture. However, maximizing the Fluorine-18 yield requires a final extraction energy between 11 MeV and 18 MeV. The proposed linear accelerator is modular, allowing for energy upgrades without modifying the upstream injector, LEBT, or RFQ [8].

To reach this higher energy in the future, there are two upgrade options:

- **Adding a Second DTL Tank:** A second IH-DTL cavity is installed immediately after the existing 7.0 MeV tank. This reuses the original equipment but requires a new inter-tank matching section—consisting of magnetic quadrupoles and an RF re-bunching cavity—to manage the beam transition between the two tanks [8].
- **Replacing the DTL Tank:** The existing 0.82 m DTL is replaced with a single, longer tank designed to reach 11 MeV to 18 MeV. Similar to the AccSys PULSAR [17], this method avoids complex inter-tank matching, but it requires building a new cavity and installing a larger RF power amplifier.

5 Conclusion

This report outlined the clinical necessity and technical architecture for a localized medical isotope production facility at SLRI. To address the severe transit-decay losses of Fluorine-18 in northeastern Thailand, the study first reviewed the nuclear requirements for PET radiotracers and analyzed the structural layouts of established global compact linear accelerators.

Following this review, the report successfully established the conceptual design layout for a 7 MeV proton linear accelerator. The proposed beamline integrates an ECRIS, a 325 MHz RFQ, and an IH-DTL within a compact 5.5 m footprint. By delivering an 18.0 mA peak proton beam, this configuration provides a practical and space-efficient solution for daily regional isotope manufacturing.

The adopted modular architecture also secures a clear upgrade path for the facility. The system can accommodate future structural additions to reach extraction energies between 11 MeV to 18 MeV, which will maximize isotope yields as regional medical demand grows.

6 Target Users of the Report

This technical report is written for personnel involved in developing the SLRI compact proton linac. The primary users include:

- SLRI staff to evaluate the conceptual design and approve the physical prototyping phase.
- SLRI staff using the report as material to write other technical reports or research proposals.
- Physicists and engineers to use the baseline parameters for beam dynamics simulations and mechanical modeling.
- Other interested readers to review the proposed beamline architecture and provide technical feedback.

References

[1] S. Cherry, J. Sorenson, and M. Phelps, *Physics in Nuclear Medicine*. ClinicalKey 2012, Elsevier Health Sciences, 2012.

[2] Chulabhorn Hospital, "Chulabhorn hospital." https://chulabhornhospital.cra.ac.th/Medical/. Accessed: 2026-07-11.

[3] T. Kaewchur, B. Khiewvan, W. Chamroonrat, *et al.*, "Thai national guideline for nuclear medicine investigation in movement disorders: Nuclear medicine society of thailand, the neurological society of thailand, and thai medical physicist society collaboration," *Asia Oceania Journal of Nuclear Medicine and Biology*, vol. 12, no. 1, pp. 60–73, 2024.

[4] D. Suttho, K. Koompai, N. Jantaruk, W. Kittichai, P. Chusorn, S. Pornprasert, and et al., "Establishment of national diagnostic reference levels for administered activity in diagnostic nuclear medicine in thailand," *Journal of Nuclear Medicine Technology*, vol. 52, no. 2, pp. 158–162, 2024.

[5] International Atomic Energy Agency, "Nuclear data for charged-particle production of medical radioisotopes: $^{18}\mathrm{O}(\mathrm{p,n})^{18}\mathrm{F}$." https://nds.iaea.org/medical/o8p18f0.html, 2021. Accessed: 2026-07-08; Updated Sep. 2021.

[6] International Atomic Energy Agency, "Cyclotron produced radionuclides: Physical characteristics and production methods," Technical Reports Series 468, International Atomic Energy Agency, 2009. Chapter 2.18: Fluorine-18.

[7] Pantechnik S.A., *SISLI 2.45 GHz ECR Ion Source: Technical Specifications and Operations*, 2024. Accessed: 2026-07-09.

[8] T. P. Wangler, *RF Linear Accelerators*. John Wiley & Sons, 2 ed., 2008.

[9] R. W. Hamm and M. E. Hamm, *Industrial Accelerators and Their Applications*. World Scientific, 2012. Comprehensive reference for the parameters and operational advantages of ECRIS and RFQ/DTL structures in commercial and medical environments.

[10] R. W. Hamm and M. E. Hamm, "How to create a business out of manufacturing linacs," in *Proceedings of LINAC 2006*, (Knoxville, Tennessee, USA), pp. 549–553, 2006. Details the commercial development of the AccSys PULSAR RFQ+DTL linac systems specifically designed for PET radiopharmaceutical production.

[11] J. F. Ziegler, M. D. Ziegler, and J. P. Biersack, "Srim – the stopping and range of ions in matter (2010)," *Nuclear Instruments and Methods in Physics Research Section B: Beam Interactions with Materials and Atoms*, vol. 268, no. 11-12, pp. 1818–1823, 2010.

[12] T. Thuillier, "Electron cyclotron resonance ion sources - i," in *Proceedings of the CERN Accelerator School (CAS 2012): Ion Sources*, (Geneva, Switzerland), CERN, 2012.

[13] D. Leitner and C. Lyneis, *ECR Ion Sources*, ch. 11, pp. 203–231. John Wiley & Sons, Ltd, 2004.

[14] R. Geller, *Electron Cyclotron Resonance Ion Sources and ECR Plasmas*. Routledge, 1 ed., 1996.

[15] T. P. Wangler, *RF Linear Accelerators*. John Wiley & Sons, 2nd ed., 2008.

[16] J. Qiao, N. Yan, Z. Huang, Y. Zhong, J. Wang, X. Xie, Y. Pu, and W. Hu, "Physical design of a compact injector for synchrotron-based proton therapy," *Frontiers in Physics*, vol. 11, p. 1201158, 2023.

[17] AccSys Technology, Inc., "Pulsar™ system for pet isotope production," 2026. Commercial product specifications.

[18] J. Feuchtwanger, V. Etxebarria, J. Portilla, J. Jugo, I. Arredondo, I. Badillo, E. Asua, N. Vallis, M. Elorza, B. Alberdi, *et al.*, "New generation compact linear accelerator for low-current, low-energy multiple applications," *Applied Sciences*, vol. 12, no. 9, p. 4118, 2022.

[19] H. Kumada, F. Naito, K. Hasegawa, H. Kobayashi, T. Kurihara, K. Takada, T. Onishi, H. Sakurai, A. Matsumura, and T. Sakae, "Development of linac-based neutron source for boron neutron capture therapy in university of tsukuba," *Plasma and Fusion Research*, vol. 13, p. 2406006, 2018.

[20] H. Kumada, F. Naito, T. Kurihara, M. Sato, T. Shibata, A. Takagi, T. Sugimura, *et al.*, "Current development status of the linac-based bnct device of the ibnct tsukuba project," in *International Conference on Accelerators for Research and Sustainable Development: From Good Practices Towards Socioeconomic Impact*, International Atomic Energy Agency (IAEA), 2022.

[21] Y.-J. Lu, Z.-Z. Zhang, Y.-Z. Chong, Y.-H. Liu, J. Pan, C. Huang, Q. Sun, Z.-Q. Liu, X.-Y. Zhu, Y. Shao, *et al.*, "A review of planned, ongoing clinical studies and recent development of bnct in mainland of china," *Cancers*, vol. 15, no. 16, p. 4060, 2023.

[22] Pantechnik, *HiQ 60 ECRIS Source and Extraction System Technical Specifications and Engineering Layout*. Pantechnik Particle Accelerators and Ion Sources, Bayeux, France, 2026. Technical Document No. HiQ60_V02.

[23] U. Ratzinger, H. Hähnel, R. Tiede, J. Kaiser, and A. Almomani, "Combined zero degree structure beam dynamics and applications," *Physical Review Accelerators and Beams*, vol. 22, no. 11, p. 114801, 2019.

[24] P. Strehl, *Beam Instrumentation and Diagnostics*. Berlin, Heidelberg: Springer Science & Business Media, 2006.